

Three-dimensional structure and cytokine distribution of platelet-rich fibrin

Meng-Yi Bai,^{I,IV} Ching-Wei Wang,^I Jyun-Yi Wang,^I Ming-Fang Lin,^{II} Wing P. Chan^{III,*}

^IGraduate Institute of Biomedical Engineering, National Taiwan University of Science and Technology, Taipei 10607, Taiwan ^{II}Department of Radiology, Wan Fang Hospital, Taipei Medical University, Taipei 116, Taiwan. ^{III}Department of Radiology, School of Medicine, College of Medicine, Taipei Medical University, Taipei 110, Taiwan. ^{IV}Adjunct appointment to the Department of Biomedical Engineering, National Defense Medical Center, Taipei 116, Taiwan.

OBJECTIVES: Previous reports have revealed that several cytokines (including platelet-derived growth factor-BB, transforming growth factors- β 1 and insulin-like growth factor-1) can enhance the rate of bone formation and synthesis of extracellular matrix in orthopaedics or periodontology. This study aimed to determine the concentration of cytokines within platelet-rich fibrin microstructures and investigate whether there are differences in the different portions of platelet-rich fibrin, which has implications for proper clinical use of platelet-rich fibrin gel.

METHODS: Whole blood was obtained from six New Zealand rabbits (male, 7 to 39 weeks old, weight 2.7-4 kg); it was then centrifuged for preparation of platelet-rich fibrin gels and harvest of plasma. The resultant platelet-rich fibrin gels were used for cytokine determination, histological analyses and scanning electron microscopy. All plasmas obtained were subject to the same cytokine determination assays for the purpose of comparison.

RESULTS: Cytokines platelet-derived growth factor-BB and transforming growth factor- β 1 formed concentration gradients from high at the red blood cell end of the platelet-rich fibrin gel ($p=1.88 \times 10^{-5}$) to low at the plasma end ($p=0.19$). Insulin-like growth factor-1 concentrations were similar at the red blood cell and plasma ends. The porosities of the platelet-rich fibrin samples taken in sequence from the red blood cell end to the plasma end were $6.5\% \pm 4.9\%$, $24.8\% \pm 7.5\%$, $30.3\% \pm 8.5\%$, $41.4\% \pm 12.3\%$, and $40.3\% \pm 11.7\%$, respectively, showing a gradual decrease in the compactness of the platelet-rich fibrin network.

CONCLUSION: Cytokine concentrations are positively associated with platelet-rich fibrin microstructure and portion in a rabbit model. As platelet-rich fibrin is the main entity currently used in regenerative medicine, assessing cytokine concentration and the most valuable portion of PRF gels is essential and recommended to all physicians.

KEYWORDS: Biomaterial; Cytokine; Platelet-Rich Fibrin (PRF).

Bai MY, Wang CW, Wang JY, Lin MF, Chan WP. Three-dimensional structure and cytokine distribution of platelet-rich fibrin. Clinics. 2017;72(2):116-124

Received for publication on September 1, 2016; First review completed on November 5, 2016; Accepted for publication on November 28, 2016

*Corresponding author. E-mail: wingchan@tmu.edu.tw

INTRODUCTION

Platelet-rich fibrin (PRF) is a second generation platelet-containing biomaterial with potential applications in wound healing. Unlike the first generation of platelet-rich products, such as platelet-rich plasma (PRP), PRF does not require the addition of an anticoagulant (such as ethylenediaminetetraacetic acid [EDTA]) during the initial drawing of blood, nor calcium chloride nor bovine thrombin to induce polymerization (1,2). PRF traps platelets and platelet cytokines in a fibrin gel. Its multitude of cytokines at concentrations significantly higher than the baseline blood levels stimulates autologous regeneration (3). Articular cartilage repair (4-6),

regeneration after oral and maxillofacial surgery (7-9), and wound healing (10-12), all depend on the presence of cytokines that stimulate the migration and proliferation of cells within the affected part of the body. Quantification of the platelet cytokines in PRF is essential to evaluating its efficacy as a biomaterial for regenerative medicine.

The ultrastructure and fibre thickness of rabbit PRF are similar to those of human fibrin (13). Thus, in a previous study, to explore the potential use of PRF gel in regenerative medicine, we used an experimental rabbit model to investigate the regeneration of articular cartilage defects in the knee; this model consisted of autologous implantation of PRF and minced cartilage fragments into injured knees (4). Although the study indicated that the observed healing might be due to the release of cytokines from the autologous PRF, no qualitative or quantitative evidence of platelet cytokines in the PRF was presented, limiting the preclinical elucidation of the study and its translation to clinical treatment of articular cartilage injury.

Dohan and coworkers (14) quantified the cytokine concentrations in the three layers formed by centrifugation of

This is an Open Access article distributed under the terms of the Creative Commons Attribution Non-Commercial License (<http://creativecommons.org/licenses/by-nc/3.0/>) which permits unrestricted non-commercial use, distribution, and reproduction in any medium, provided the original work is properly cited.

No potential conflict of interest was reported.

DOI: 10.6061/clinics/2017(02)09



blood in a collection tube (red blood cells [RBC], PRF, and plasma), but they considered the middle layer (i.e., the PRF gel) to be the only potential cytokine source for clinical practice and therefore focused on measuring the concentration of platelet cytokines in PRF gels. In another study, it was shown that fibrin architecture and leukocyte content influence cytokine release from four different families of platelet concentrates, not including PRF (15,16). The abovementioned findings inspired us to ask whether cytokines are concentrated and evenly distributed in PRF gel, as this is the main entity currently used in regenerative medicine, for example, in dentistry (17,18).

In this study, we focused on PRF gel because this is the only autologous family of platelet concentrates without the addition of foreign reagent and able to reserve and release cytokines in a controlled manner (19). Three platelet cytokines (platelet-derived growth factor-BB: PDGF-BB, transforming growth factor-beta 1: TGF- β 1 and insulin-like growth factor 1: IGF-1) were chosen for analyses because their biological activities during initial healing are well understood (20). Although research on human cytokines quantification has been widely reported (21-25), we approached the issue differently in this study by quantifying cytokines obtained from districted PRF, not global PRF, in rabbits. It is because of the unexpected discovery of an uneven distribution of cytokines in our previous study to elucidate the potential use of PRF gel in regenerated articular cartilage defects in rabbits' knees. We therefore raised two questions: first whether these cytokines are indeed concentrated in the PRF gel rather than in plasma, and second, if so, whether they are evenly distributed in the fibrin network of the PRF gel. These questions led us to determine the cytokine content of PRF and its relationship with the three-dimensional fibrin network structure.

MATERIALS AND METHODS

Preparation of PRF gel and matrix

Six New Zealand rabbits (male, 7 to 39 weeks old, weight 2.7-4 kg) were used for the preparation of PRF gels. The animal breeding practices and animal use protocol were approved by the Institutional Animal Care and Use Committee (IACUC) at Taipei Medical University (certificate no. LAC-101-0300). The rabbits were maintained according to the regulations of the IACUC at our institution, where they were housed. All experiments were performed in accordance with the replace, reduce, and refine principles outlined in the IACUC guidelines. The number of animals was the minimum required to obtain statistically valid results. The sample size per group was calculated based on an estimated between-group difference of 0.5, assuming a two-sided confidence interval of 95% and a variance of 0.5.

PRF was prepared using the protocol that was described for the first time internationally by Dohan et al. in 2006 (26) with slight modifications to improve reproducibility. Because only rabbits above 3 kg body-weight have large enough ear veins for venipuncture, these larger rabbits were placed in a restraining device to facilitate the drawing of blood (Figure 1a). In addition, xylene (ACS reagent, J. T. Baker, Phillipsburg, NJ, USA) was applied to the skin over the ear vein to dilate the vessel and assist in locating the vein. Five millilitres of blood were drawn from the ear vein (Figure 1b) with a no. 21 gauge butterfly needle, immediately transferred to an 8-mL sterile plastic tube (without anticoagulant, Vacuette[®] tube, 2 mL Z no additive, item no. 455071), and centrifuged at

3000 rpm for 10 min in a DSC-200A-2 tabletop centrifuge (Digisystem, Laboratory Instruments Inc., Taipei, Taiwan). It is noteworthy that only the venous blood could successfully produce the PRF gel after it was subject to centrifugation (Figure 1b-c, confirmation that blood was drawn from the rabbit auricular vein, not from the central ear artery). A pair of forceps was used to remove the middle layer (the whole PRF gel, Figure 1d) from the top layer (plasma) and bottom layer (RBC). The plasma was then harvested and stored in an Eppendorf tube (Avant[®] microcentrifuge tube, 1.7 mL, certified free of RNase/DNase, human DNA, Pyrogen, PCR inhibitors) for the following analyses. A representative PRF gel prepared from centrifugation of 5 mL of whole blood is shown in Figure 1d. Before placing the PRF sample in the freezer, the surface adsorbing RBC layer fluid had to be completely drained away to avoid interference with the cytokine determination assays. The PRF (a pale yellow elastic gel-like strip) was frozen at -20°C for 30 min and then transferred to another freezer at -80°C for storage until the cytokines were quantified. This gradual freezing protocol mimics the protocol for freezing cells to avoid denaturation of cytokine proteins as cytokine levels can be decreased by improper handling and storage of samples (27).

Each of the six PRF samples was divided into three segments for cytokine quantification. Normally, the pointed tip on the RBC end was trimmed off, as RBC contamination strongly influenced cytokine determination using the spectrometer. Therefore, cytokines from the RBC layer were excluded. Then, cytokine activation was conducted in 4-(2-hydroxyethyl)-1-piperazineethanesulfonic acid (HEPES, $\geq 99.5\%$, Sigma-Aldrich, St Louis, MO, USA, pH 7.2-7.6). Cytokine concentration was measured using sandwich-type ELISA kits (nos. MBS165883, MBS165545, and MBS704445, MyBiosource, Inc., San Diego, CA, USA) according to the manufacturer's instructions. After the exudate was removed from the defrosted PRF gel, the remaining white PRF matrix was fixed in 10% formalin (Sigma-Aldrich) for 22 h and dehydrated in a graded ethanol series (70% to 100%) for the following preparation of histological specimens.

Histological and scanning electron microscopic analysis

The PRF sample was fixed, dehydrated and placed in a tissue cassette and embedded in paraffin wax. Infiltration of paraffin into the porous tissue maintains the intrinsic morphology of the tissue and solidifies the sample to allow fine sectioning. The sample was divided into seven segments (Figure 2a-c), then cut into 3-5 μm sections for histological analyses. The RBC end and plasma end of the PRF were similar and easily confused during this preparation of histological samples. Sample orientation errors were avoided by labelling. The tissue sections were mounted on slides, stained with haematoxylin-eosin or Masson's trichrome stain, viewed and photographed under an optical microscope (28). The compactness of the fibrin network (i.e., porosity, [n]) was measured directly by scanning electron microscopy (SEM) using ImageJ software (NIH, Bethesda, MD, USA). Porosity $[n] = A_p/A_t \times 100\%$, where A_p denotes the measured total area of the pores in each SEM image and A_t is the total area of an SEM image.

All protocols of histological and SEM analyses for the animal rabbit model were developed for this PRF sample and were slightly modified from the typical tissue preparation

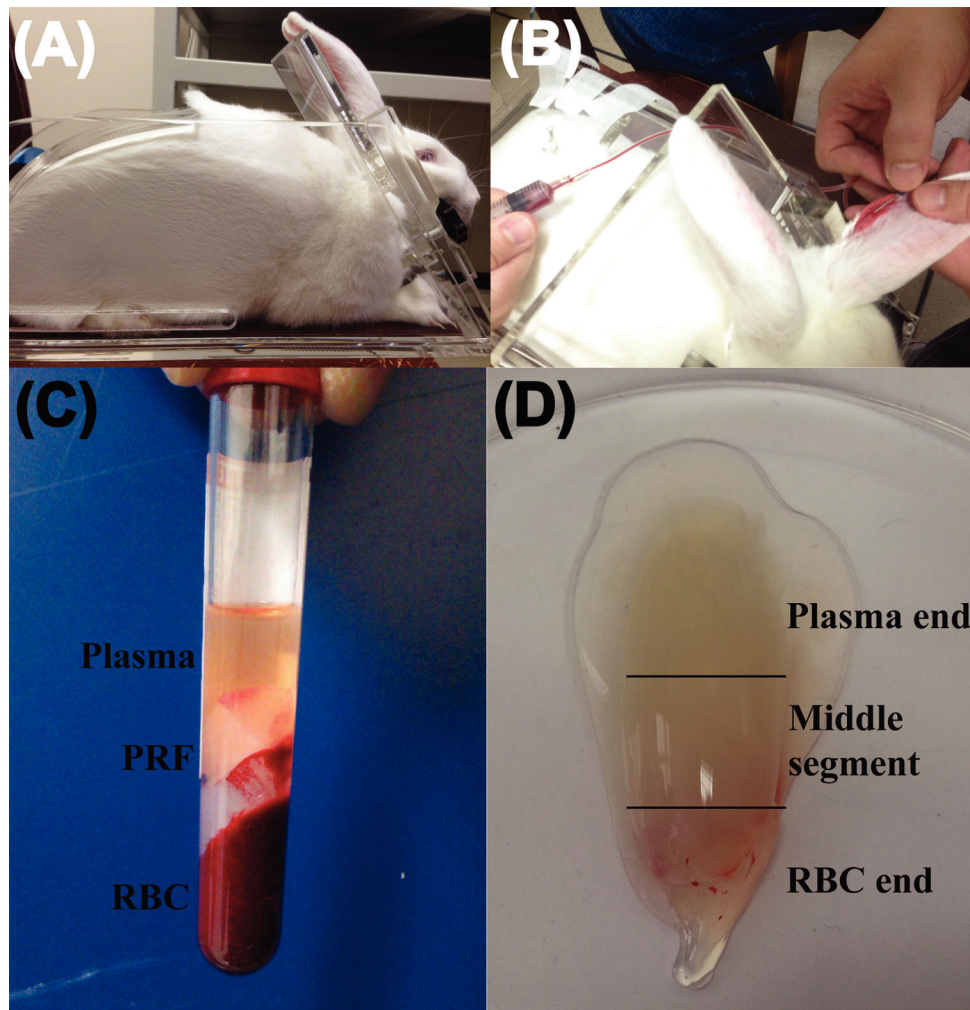


Figure 1 - Preparation of platelet-rich fibrin (PRF) gel using blood from New Zealand rabbits. (A) A rabbit is placed in a restraining frame. (B) Blood is drawn from an ear vein. (C) A 5-mL blood sample is separated into three layers by centrifugation at 3000 rpm for 10 min. (D) A PRF gel forms between the plasma layer (top) and the red blood cell (RBC) layer (bottom).

method for light microscopy. Optical microscopy and SEM were used in a complementary fashion, as they have different levels of resolution for inspecting the fibrin microstructure (the resolution of the optical microscope falls within the μm range and that of the SEM can be in nm). To prevent charge accumulation and damage to tissue sections during SEM examination, approximately 80 Å of platinum was deposited on the tissue sections using a sputter coater. SEM images were acquired using a field-emission scanning electron microscope (FESEM, Model JSM-5600, JEOL, Tokyo, Japan) operated at an accelerating voltage of 15 kV. Serial images were aligned sequentially in three-dimensional space and visualized three-dimensionally with Fiji and TrakEM2 software (29,30). In a typical procedure, serial slides can be manually aligned by setting up a number of pairs of corresponding control points to the same (x, y) location for consecutive images z_i and z_{i+1} , and the pairs of images and paired-sets of control points are then given to semi-automatic software for image alignment. Fully automatic registration of biological images is then possible as demonstrated by the software - TrakEM2 (29,30). The average diameters of the fibrin fibres were obtained by averaging diameters directly measured in the SEM images of ~ 30 samples.

Statistical analysis

The concentrations of cytokines from six rabbits are expressed as the mean \pm SD for each type of cytokine. Student's *t*-test was used to compare results for PRF and plasma (the control). $P < 0.05$ was considered statistically significant. Excel[®] (Microsoft, Seattle, WA, USA) was used for statistical analysis.

RESULTS

Cytokine measurement

Figure 3 shows data obtained from all six rabbits. PDGF-BB and TGF- β 1 formed quasi-gradients of concentration from high at the RBC end (PRF1, $p = 1.88 \times 10^{-5}$ compared with the level in plasma) to low at the plasma end (PRF3, $p = 0.19$). IGF-1 concentrations were similar at the RBC and plasma ends (no statistical significance was observed).

Histological and SEM observations

Compactness and porosity in the PRF tended to be non-uniform (Figure 4). The fibrin network (see the red area indicated by the green arrowheads) closest to the RBC layer had particularly small pores and an ultra-compact structure

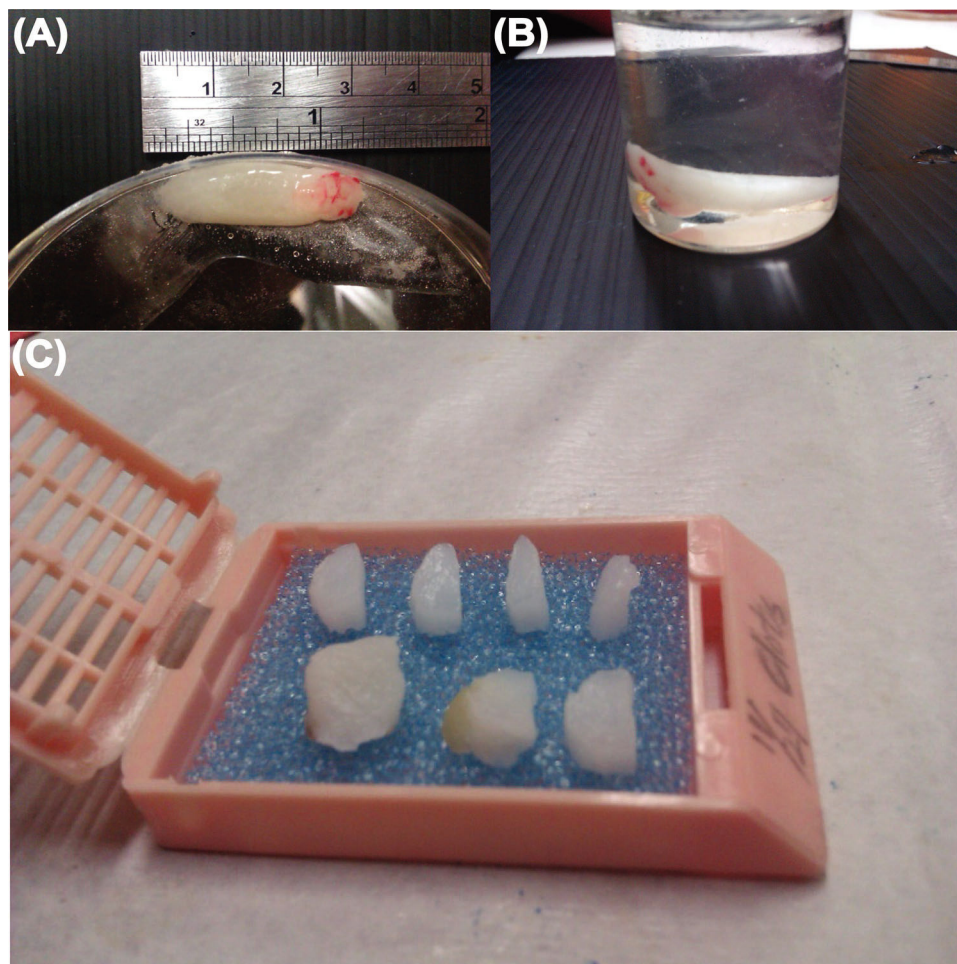


Figure 2 - Photographs showing (A) a defrosted PRF gel, (B) a PRF gel fixed in 10% formalin for 22 h, and (C) the fixed PRF gel embedded in paraffin, divided into 7 segments and sent for paraffin sectioning. The two ends of the PRF gel were discarded due to distortion.

with many incorporated platelets (see the blue spots indicated by the white arrowheads, the PRF section observed in Figure 4a corresponds to PRF1 shown in Figure 3) and that closest to the plasma layer had larger pores and a less compact structure (the PRF section observed in Figure 4e corresponds to PRF3 shown in Figure 3, the remaining images, i.e., Figure 4b-d, correspond to PRF2 shown in Figure 3). The porosities of these PRF samples taken in sequence from the RBC end to the plasma end were $6.5\% \pm 4.9\%$, $24.8\% \pm 7.5\%$, $30.3\% \pm 8.5\%$, $41.4\% \pm 12.3\%$, and $40.3\% \pm 11.7\%$ (Figure 5, as illustration of sample sites shown in Figure 6a), indicating a gradual decrease in the compactness of the PRF network.

SEM images showed that the fibrin fibres in the five segments of a representative PRF sample (images taken sequentially from the RBC end to the plasma end; Figure 6a) had average diameters of 116 ± 37 , 116 ± 39 , 123 ± 37 , 124 ± 38 , and 140 ± 39 nm, respectively. In addition, because robust and fully automatic 3D registration of serial-section microscopic images is critical for detailed anatomical reconstruction of large biological specimens, such as the case of PRF histology shown above. This construction image can help with providing more information about the essence of platelet-rich fibrin (ePRF) to gain new structural insights. On reconstructing the two-dimensional SEM images and viewing from above, the three-dimensional reconstruction

image of the fibrin matrix was dense and similar in appearance to medical gauze (Figure 7a). From the side-view, the compactness decreased and porosity increased along the longitudinal axis of the PRF sample from the RBC end to the plasma end (Figure 7b).

DISCUSSION

This study confirms that platelet cytokines are indeed trapped in PRF gel but contradicts the hypothesis of Mosesson et al. (31,32) that the trapped platelet cytokines are evenly distributed throughout the fibrin network. The formation of a three-dimensional fibrin network resulted in the incorporation of cytokines into its mesh architecture. We propose that fibrinogen and thrombin concentrations are higher at the RBC end of a PRF sample, possibly because of the force of centrifugation. Our results agree with those of Ryan and Wang (33, 34), who demonstrated that a higher concentration of thrombin results in the generation of fibrin with a smaller diameter and that these smaller fibrin fibres tend to pack more tightly, such that the porosity is lower. Our results provide clinically useful information that could support the development of improved therapeutic interventions, as the potential curative effect of PRF arises mainly from its high concentration of incorporated cytokines.

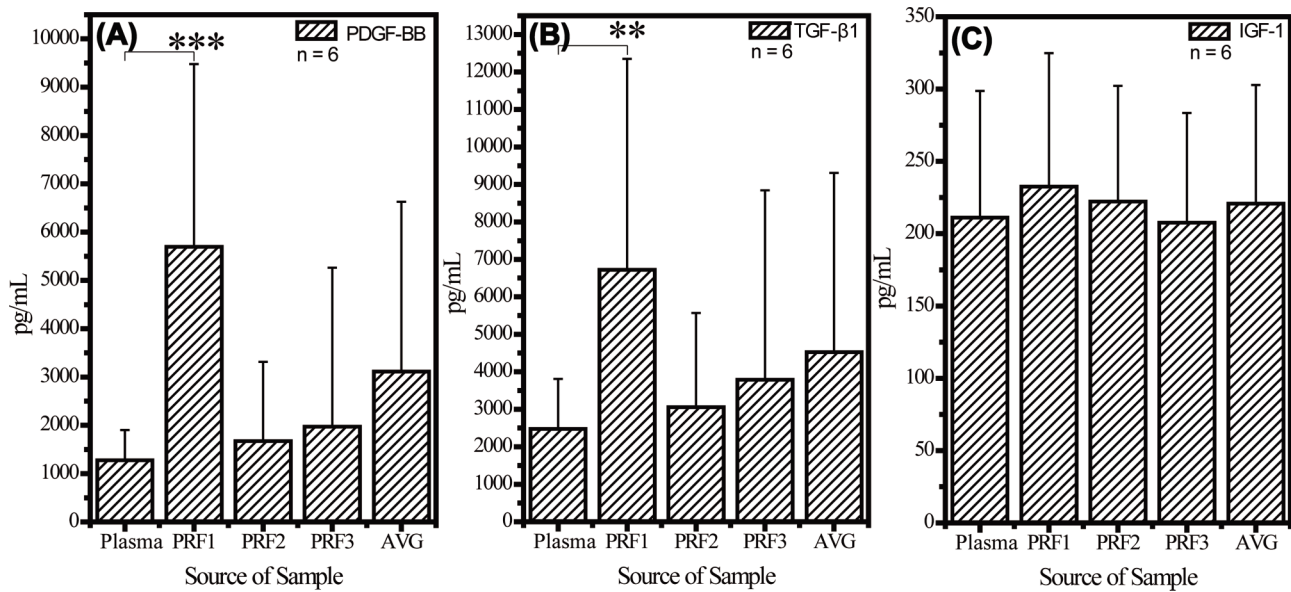


Figure 3 - Cytokine quantification assay of (A) PDGF-BB, (B) TGF-β1, and (C) IGF-1 in PRF gel. All values are expressed as the mean \pm SD. The RBC end, middle segment, and plasma end of the PRF clot are labelled PRF1, PRF2, and PRF3, respectively. AVG is the average of the PRF1, PRF2 and PRF3 values. Concentrations of PDGF-BB and TGF-β1 in PRF1 were always two to five times that in PRF3, but the concentration of IGF-1 in PRF1 did not differ significantly from that in PRF3. p value < 0.01 is labelled **, and p value < 0.001 is labelled ***. All statistical results are with respect to the group of plasma.

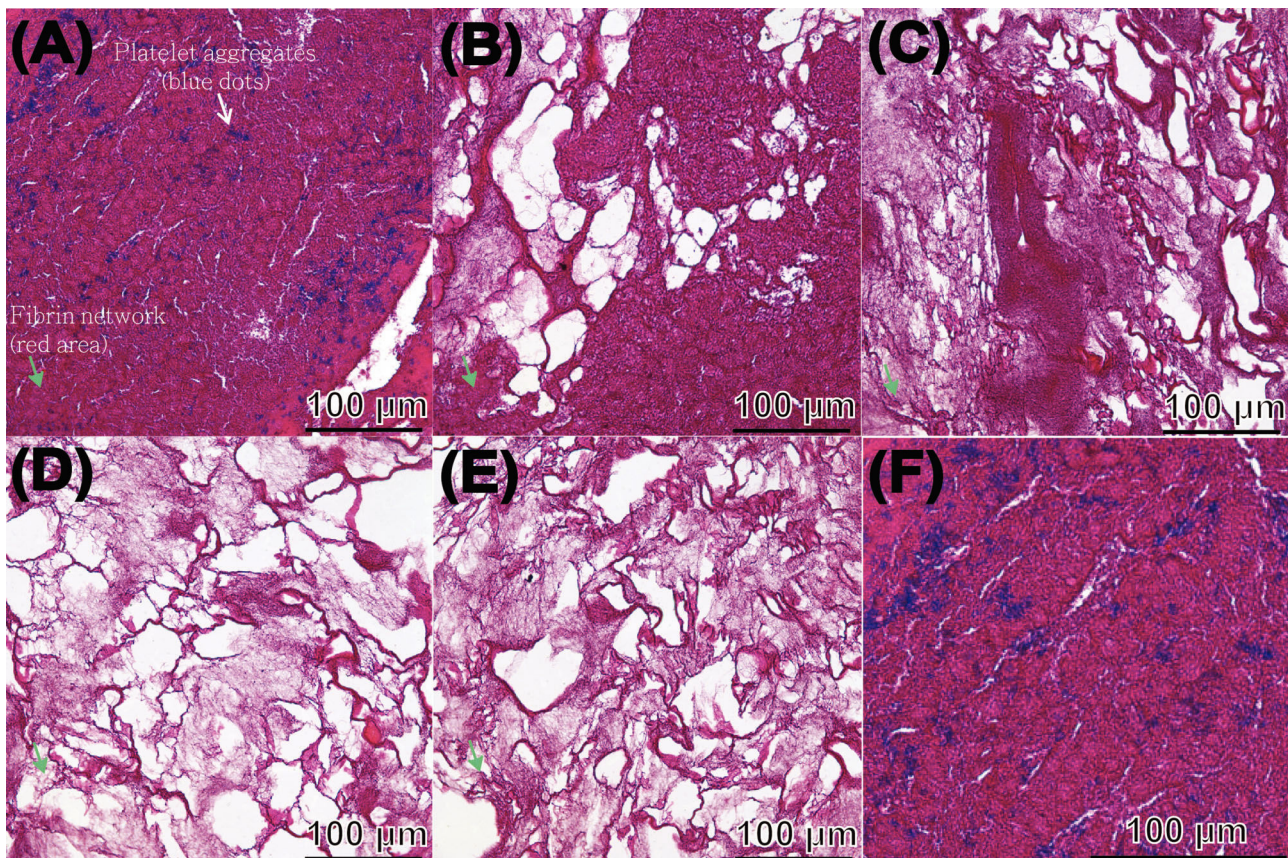


Figure 4 - The five segments obtained from the PRF sample shown in Figure 2 were used for histological analysis, and sections were stained with Masson's trichrome. Sections from the RBC end (A), middle segment (B-D), and plasma end (E) of the PRF show a decrease in compactness and increase in porosity as the view of the PRF gel shifts from the RBC end to the plasma end. A micrograph (F) taken at high magnification from (A), revealing finer structural details.

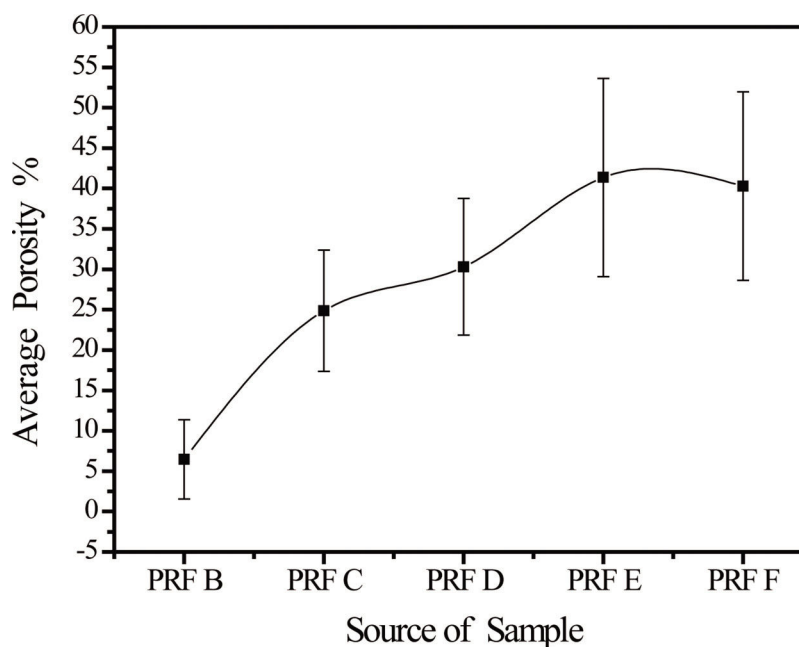


Figure 5 - Statistics concerning the porosity of the PRF specimens shown in Figure 2 (for interpretation of the sample labelling, please refer to Figure 6a).

Images of histologically stained PRF show fibrin networks with varying degrees of compactness. To the best of our knowledge, the three-dimensional fibrin network of leukocyte-PRF (L-PRF) first reported by Dohan et al. in 2006 is the catalyst for the incorporation of cytokines into the mesh architecture. However, this idea is based on theoretical computer modelling of a PRF clot, not empirical evidence. Our three-dimensional representation of the PRF microstructure reconstructed from a series of two-dimensional SEM images shows a dense fibrin matrix with surface morphology similar to that of medical gauze. This tangled fibrous architecture, in contrast to the architecture of the first-generation platelet concentrate commonly known as PRP, is responsible for the slower release of growth factors and the entrapment of more platelets inside the gel (21,35). Our findings suggest that the gradient distribution of cytokines in PRF gel is strongly related to its three-dimensional structure, especially the porosity and compactness of the fibrin network. Although this structure-cytokine gradient relationship seems tied to the conditions of PRF preparation, such as types of tube for collecting blood, types of centrifuge, centrifugal force and duration of centrifugation (36), it has not been possible to establish this relationship by conducting systematic empirical investigation because of the narrow window for successful *in vivo* preparation of PRF when the L-PRF technique was applied to an animal (rabbit) model. However, *in vitro*, Ryan and Wang (33,34) have shown that adding higher concentrations of thrombin results in the generation of fibrin with a smaller diameter.

When a whole blood sample is centrifuged, a gelled membrane (the buffy coat layer) forms between the RBC layer and the plasma layer. The buffy coat contains most of the platelets, which are activated during centrifugation. The surface of these activated platelets is known to contain glycoprotein IIb/IIIa, which is a receptor for binding the soluble fibrinogen protein in fluid (37). The activated platelets also stimulate the formation of thrombin and induce the subsequent

polymerisation of fibrinogen to form fibrin molecules. These adhere to one another and then become assembled into long fibrils. The formation of this fibrin gel is generally determined by the balance between the lateral aggregation of fibrinogen monomers and the rate of fibrinopeptide cleavage (38). At a high concentration of thrombin, the rate of fibrinopeptide cleavage, with simultaneous creation of many branch-points, exceeds the rate of lateral aggregation of fibrinogen monomers, giving rise to a network of thin fibres. Therefore, we propose that the concentration of fibrinogen and thrombin at the RBC end of the PRF gel is higher than that in the rest of the PRF, possibly because of the effects of density-gradient centrifugation and incorporation of platelets (Figure 4a). This provides a microenvironment conducive to the formation of a network composed of small but densely packed fibres. Our results (Figures 4–7) confirmed that the fibrin fibres at the RBC end of the PRF clot were more tightly packed (of higher density and smaller diameter) and therefore had lower porosity, so the fibres trapped more platelets, which exhibited a locking effect on the cytokines and thrombin. Conversely, the thrombin components required for conversion of fibrinogen to fibrin pass through the densely packed fibrin network from the RBC end to the plasma end of the PRF gel, generating a loosely packed fibrin network at the plasma end.

The distributions of PDGF-BB and TGF- β 1, but not IGF-1, in the PRF gel were quasi-graded, and their concentrations were much higher in the PRF gel than in the plasma. Our preliminary results indicated that this effect is a combination of two factors: 1) an extrinsic factor attributed to the fibrin gel structure; and 2) an intrinsic factor attributed to the molecular structure of different cytokines. All of these cytokines were soluble and therefore should concentrate in plasma after centrifugation. However, the highest concentrations of the cytokines were at the RBC end of the gel, implying that the cytokines were stoichiometrically trapped in the PRF gel. This was a process akin to harvesting fish by casting a net

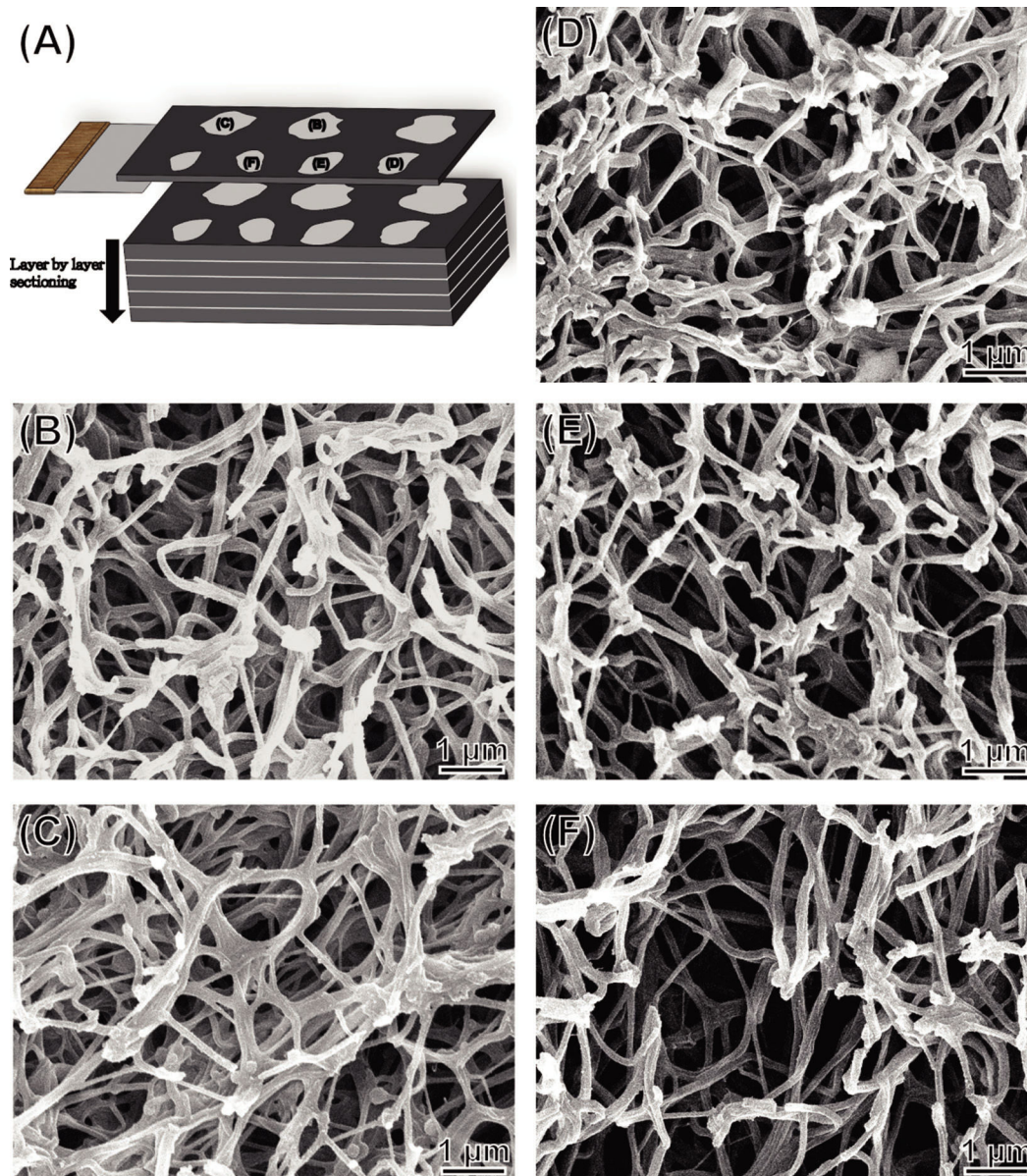


Figure 6 - (A) Diagrammatic view of a sectioned PRF gel and (B–F) SEM images of the series of PRF sections shown in Figure 2. Labels in (A) indicate the five segments of the PRF sample observed in the SEM micrographs.

into water; the process depended on the size of the mesh, which if small could remove more large granules or molecules, such as platelets, PDGF-BB (31 kDa) (39), and TGF- β 1 (25 kDa) (40). Because of its much lower molecular weight, IGF-1 (7 kDa) was less likely to be incorporated and retained in the fibrin matrix (41), which is consistent with the observation of Dohan et al. that IGF-1 is principally a circulating molecule (13), tending to concentrate in the upper part of the tube after centrifugation. We believe that this determination of the cytokine content of PRF produced from L-PRF technique applied to rabbit model and its relationship with the three-dimensional fibrin network structure will have a positive impact on the development of PRF products with higher clinical efficacy, such as surgical implantation of PRF in repairing articular cartilage or implanting a tooth (42) as patients desire a smaller incision, faster identification of the defect, and fewer surgeries.

In conclusion, the concentration of cytokines in a PRF gel is not uniform. The RBC end of a PRF gel contains the highest concentration of platelets and cytokines, which was thus defined as the essence of platelet-rich fibrin (ePRF). Three factors govern this distribution of cytokines: 1) the platelet distribution (which determines the concentration of thrombin); 2) the three-dimensional fibrin structure (which differs in porosity and compactness); and 3) the molecular weights of the cytokines. The structure of the PRF gel and its related cytokine distribution can inform the decision to use PRF clinically, as the efficacy of PRF is theoretically mainly dependent on the high concentrations of growth factors found within PRF compared with whole blood, which is similar to other platelet-rich products. A more extensive animal study and institutional review board (IRB)-approved human-subject study is currently comparing and extrapolating the findings of our work.

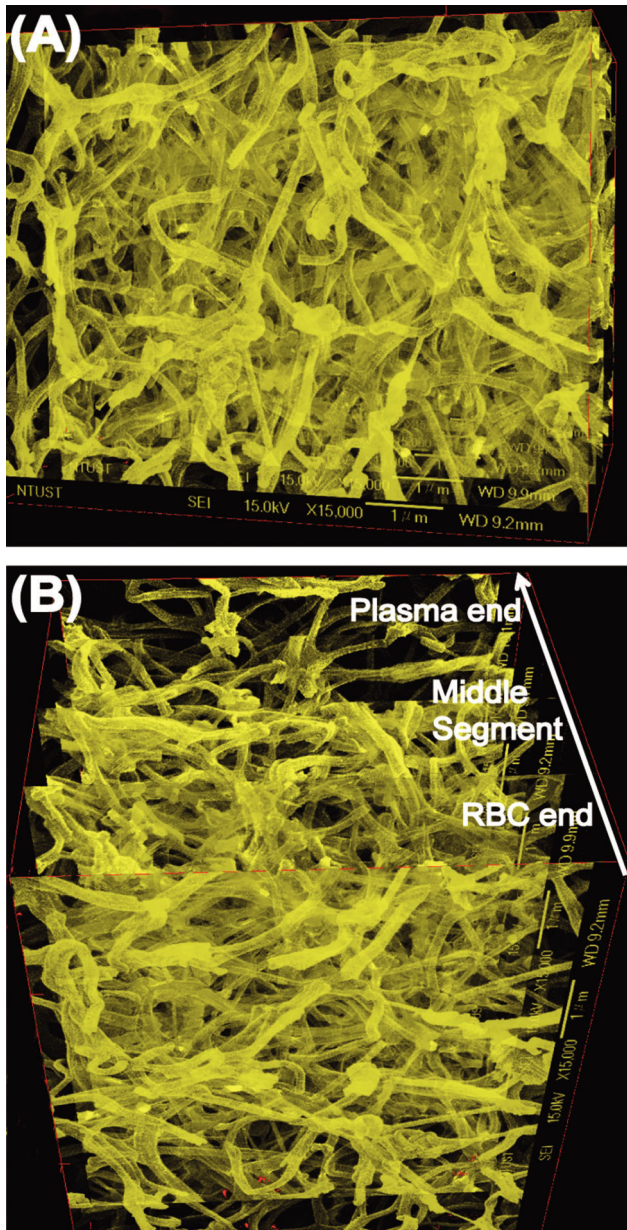


Figure 7 - Three-dimensional image constructed from the SEM images shown in Figure 6. (A) Top view showing the PRF gel from the RBC end, and (B) side view showing the cross-section of the PRF gel. An arrow indicates the direction of gradually decreasing compactness and increasing porosity of the PRF microstructure from the RBC end to the plasma end.

ACKNOWLEDGMENTS

This work was supported by grants from the Taipei Medical University–National Taiwan University of Science and Technology Joint Research Program (TMU-NTUST-102-10) in Taiwan.

AUTHOR CONTRIBUTIONS

Bai MY, Lin MF and Chan WP conceived and designed the experiments. Bai MY, Wang CW, Wang JY, and Lin MF performed the experiments. Bai MY and Chan WP analyzed the data. Bai MY, Wang CW, Wang JY, Lin MF, Chan WP contributed reagents/materials/analysis tools. Bai MY wrote the paper. Wang CW, Lin MF, Chan WP revised the manuscript critically for important intellectual content.

REFERENCES

- Landesberg R, Roy M, Glickman RS. Quantification of growth factor levels using a simplified method of platelet-rich plasma gel preparation. *J Oral Maxillofac Surg.* 2000;58(3):297-300, [http://dx.doi.org/10.1016/S0278-2391\(00\)90058-2](http://dx.doi.org/10.1016/S0278-2391(00)90058-2).
- Landesberg R, Burke A, Pinsky D, Katz R, Vo J, Eising SB, et al. Activation of platelet-rich plasma using thrombin receptor agonist peptide. *J Oral Maxillofac Surg.* 2005;63(4):529-35, <http://dx.doi.org/10.1016/j.joms.2004.12.007>.
- Civinini R, Macera A, Nistri L, Redl B, Innocenti M. The use of autologous blood-derived growth factors in bone regeneration. *Clin Cases Miner Bone Metab.* 2011;8(1):25-31.
- Kuo TF, Lin MF, Lin YH, Lin YC, Su RJ, Lin HW, et al. Implantation of platelet-rich fibrin and cartilage granules facilitates cartilage repair in the injured rabbit knee: preliminary report. *Clinics.* 2011;66(10):1835-8, <http://dx.doi.org/10.1590/S1807-59322011001000026>.
- Baek HS, Lee HS, Kim BJ, Chung IK, Kim CH, Jin SM, et al. Effect of platelet-rich fibrin on repair of defect in the articular disc in rabbit temporomandibular joint by platelet-rich fibrin. *Tissue Eng Regen Med.* 2011;8(6):530-5.
- Perka C, Spitzer RS, Lindenhayn K, Sittlinger M, Schultz O. Matrix-mixed culture: new methodology for chondrocyte culture and preparation of cartilage transplants. *J Biomed Mater Res.* 2000;49(3):305-11, [http://dx.doi.org/10.1002/\(SICI\)1097-4636\(20000305\)49:3<305::CO;2-9](http://dx.doi.org/10.1002/(SICI)1097-4636(20000305)49:3<305::CO;2-9).
- Chang YC, Wu KC, Zhao JH. Clinical application of platelet-rich fibrin as the sole grafting material in periodontal intrabony defects. *J Dent Sci.* 2011;6(3):181-8, <http://dx.doi.org/10.1016/j.jds.2011.05.010>.
- Saluja H, Dehane V, Mahindra U. Platelet-Rich fibrin: A second generation platelet concentrate and a new friend of oral and maxillofacial surgeons. *Ann Maxillofac Surg.* 2011;1(1):53-7, <http://dx.doi.org/10.4103/2231-0746.83158>.
- Simonpietri A, Del CM, Vervelle A, Jimbo R, Inchingolo F, Sammartino G, Dohan Ehrenfest DM. Current knowledge and perspectives for the use of platelet-rich plasma (PRP) and platelet-rich fibrin (PRF) in oral and maxillofacial surgery part 2: Bone graft, implant and reconstructive surgery. *Curr Pharm Biotechnol.* 2012;13(7):1231-56, <http://dx.doi.org/10.2174/138920112800624472>.
- Naik B, Karunakar P, Jayadev M, Marshal VR. Role of platelet rich fibrin in wound healing: A critical review. *J Conserv Dent.* 2013;16(4):284-93, <http://dx.doi.org/10.4103/0972-0707.114344>.
- Bielecki T, Dohan Ehrenfest DM, Everts PA, Wiczowski A. The role of leukocytes from L-PRP/L-PRF in wound healing and immune defense: new perspectives. *Curr Pharm Biotechnol.* 2012;13(7):1153-62, <http://dx.doi.org/10.2174/138920112800624373>.
- Desai CB, Mahindra UR, Kini YK, Bakshi MK. Use of platelet-rich fibrin over skin wounds: Modified secondary intention healing. *J Cutan Aesthet Surg.* 2013;6(1):35-7, <http://dx.doi.org/10.4103/0974-2077.110096>.
- Pretorius E, Vieira WA, Oberholzer HM, Auer RE. Comparative scanning electron microscopy of platelets and fibrin networks of human and different animals. *Int J Morphol.* 2009;27(1):69-76.
- Dohan DM, Choukroun J, Diss A, Dohan SL, Dohan AJ, Mouhyi J, et al. Platelet-rich fibrin (PRF): A second-generation platelet concentrate. Part II: Platelet-related biologic features. *Oral Surg Oral Med Oral Pathol Radiol Endod.* 2006;101(3):E45-50, <http://dx.doi.org/10.1016/j.tripleo.2005.07.009>.
- Dohan Ehrenfest DM, Bielecki T, Jimbo R, Barbé G, Del Corso M, Inchingolo F, et al. Do the fibrin architecture and leukocyte content influence the growth factor release of platelet concentrates? An evidence-based answer comparing a pure platelet-rich plasma (P-PRP) gel and a leukocyte- and platelet-rich fibrin (L-PRF). *Curr Pharm Biotechnol.* 2012;13(7):1145-52, <http://dx.doi.org/10.2174/138920112800624382>.
- Dohan Ehrenfest DM, Bielecki T, Mishra A, Borzini P, Inchingolo F, Sammartino G, et al. In search of a consensus terminology in the field of platelet concentrates for surgical use: platelet-rich plasma (PRP), platelet-rich fibrin (PRF), fibrin gel polymerization and leukocytes. *Curr Pharm Biotechnol.* 2012;13(7):1131-7, <http://dx.doi.org/10.2174/138920112800624328>.
- Borie E, Olivé DG, Orsi IA, Garlet K, Weber B, Beltrán V, et al. Platelet-rich fibrin application in dentistry: a literature review. *Int J Clin Exp Med.* 2015;8(5):7922-9.
- Hotwani K, Sharma K. Platelet rich fibrin - a novel acumen into regenerative endodontic therapy. *Restor Dent Endod.* 2014;39(1):1-6, <http://dx.doi.org/10.5395/rde.2014.39.1.1>.
- Mazzucco L, Balbo V, Cattana E, Guaschino R, Borzini P. Not every PRP-gel is born equal. Evaluation of growth factor availability for tissues through four PRP-gel preparations: Fibrinet, RegenPRP-Kit, Plateltex and one manual procedure. *Vox Sang.* 2009;97(2):110-8, <http://dx.doi.org/10.1111/j.1423-0410.2009.01188.x>.
- Giannobile WV. Periodontal tissue engineering by growth factors. *Bone.* 1996;19(1 Suppl):23S-37S, [http://dx.doi.org/10.1016/S8756-3282\(96\)00127-5](http://dx.doi.org/10.1016/S8756-3282(96)00127-5).
- Dohan Ehrenfest DM, de Peppo GM, Doglioli P, Sammartino G. Slow release of growth factors and thrombospondin-1 in Choukroun's platelet-rich fibrin



- (PRF): a gold standard to achieve for all surgical platelet concentrates technologies. *Growth Factors*. 2009;27(1):63-9, <http://dx.doi.org/10.1080/08977190802636713>.
22. Dohan Ehrenfest DM, Bielecki T, Jimbo R, Barbé G, Del Corso M, Inchingolo F, et al. Do the fibrin architecture and leukocyte content influence the growth factor release of platelet concentrates? An evidence-based answer comparing a pure platelet-rich plasma (P-PRP) gel and a leukocyte- and platelet-rich fibrin (L-PRF). *Curr Pharm Biotechnol*. 2012;13(7):1145-52, <http://dx.doi.org/10.2174/138920112800624382>.
 23. Dohan Ehrenfest DM. How to optimize the preparation of leukocyte- and platelet-rich fibrin (L-PRF, Choukroun's technique) clots and membranes: introducing the PRF Box. *Oral Surg Oral Med Oral Pathol Oral Radiol Endod*. 2010;110(3):275-8.
 24. Dohan Ehrenfest DM, Del Corso M, Inchingolo F, Sammartino G, Charrier JB. Platelet-rich plasma (PRP) and platelet-rich fibrin (PRF) in human cell cultures: growth factor release and contradictory results. *Oral Surg Oral Med Oral Pathol Oral Radiol Endod*. 2010;110(4):418-21.
 25. Dohan Ehrenfest DM, Del Corso M, Diss A, Mouhyi J, Charrier JB. Three-dimensional architecture and cell composition of a Choukroun's platelet-rich fibrin clot and membrane. *J Periodontol*. 2010;81(4):546-55, <http://dx.doi.org/10.1902/jop.2009.090531>.
 26. Dohan DM, Choukroun J, Diss A, Dohan SL, Dohan AJ, Mouhyi J, et al. Platelet-rich fibrin (PRF): A second-generation platelet concentrate. Part I: Technological concepts and evolution. *Oral Surg Oral Med Oral Pathol Oral Radiol Endod*. 2006;101(3):e37-e44, <http://dx.doi.org/10.1016/j.tripleo.2005.07.008>.
 27. Panicker G, Meadows KS, Lee DR, Nisenbaum R, Unger E. Effect of storage temperatures on the stability of cytokines in cervical mucous. *Cytokine*. 2007;37(2):176-9, <http://dx.doi.org/10.1016/j.cyto.2007.03.006>.
 28. Jonassen JA, San Agustin J, Folliot JA, Pazour GJ. Deletion of IFT20 in the mouse kidney causes misorientation of the mitotic spindle and cystic kidney disease. *J Cell Biol*. 2008;183(3):377-84, <http://dx.doi.org/10.1083/jcb.200808137>.
 29. Schindelin J, Arganda-Carreras I, Frise E, Kaynig V, Longair M, Pietzsch T, et al. Fiji: an open-source platform for biological-image analysis. *Nat Methods*. 2012;9(7):676-82, <http://dx.doi.org/10.1038/nmeth.2019>.
 30. Cardona A, Saalfeld S, Schindelin J, Arganda-Carreras I, Preibisch S, Longair M, et al. TrakEM2 software for neural circuit reconstruction. *PLoS One*. 2012;7(6):e38011, <http://dx.doi.org/10.1371/journal.pone.0038011>.
 31. Pretorius E, Briedenhann S, Marx J, Smit E, Van Der Merwe C, Pieters M, et al. Ultrastructural comparison of the morphology of three different platelet and fibrin fiber preparations. *Anat Rec*. 2007;290(2):188-98, <http://dx.doi.org/10.1002/ar.20413>.
 32. Mosesson MW, Siebenlist KR, Meh DA. The structure and biological features of fibrinogen and fibrin. *Ann N Y Acad Sci*. 2001;936:11-30, <http://dx.doi.org/10.1111/j.1749-6632.2001.tb03491.x>.
 33. Ryan EA, Mockros LF, Weisel JW, Lorand L. Structural origins of fibrin clot rheology. *Biophys J*. 1999;77(5):2813-26, [http://dx.doi.org/10.1016/S0006-3495\(99\)77113-4](http://dx.doi.org/10.1016/S0006-3495(99)77113-4).
 34. Wang R. Effects of varying thrombin and calcium concentration on the structure, mechanical properties, and cellular compatibility of fibrin gels. Honor Thesis, Tufts University. 2012. [http://dl.tufts.edu/fileassets/tufts:UA005.019.032.00001\(date last accessed 21 February 2016\)](http://dl.tufts.edu/fileassets/tufts:UA005.019.032.00001(date%20last%20accessed%2021%20February%202016)).
 35. Dohan Ehrenfest DM, Andia I, Zumstein MA, Zhang CQ, Pinto NR, Bielecki T. Classification of platelet concentrates (Platelet-Rich Plasma-PRP, Platelet-Rich Fibrin-PRF) for topical and infiltrative use in orthopedic and sports medicine: current consensus, clinical implications and perspectives. *Muscles Ligaments Tendons J*. 2014;4(1):3-9.
 36. Dohan Ehrenfest DM, Kang BS, Del Corso M, Nally M, Quirynen M, Wang HL, et al. The impact of the centrifuge characteristics and centrifugation protocols on the cells, growth factors and fibrin architecture of a Leukocyte- and Platelet-Rich Fibrin (L-PRF) clot and membrane. Part 1: evaluation of the vibration shocks of 4 models of table centrifuges for L-PRF. *POSEIDO*. 2014;2(2):129-39.
 37. Yip J, Shen Y, Berndt MC, Andrews RK. Primary platelet adhesion receptors. *IUBMB Life*. 2005;57(2):103-8, <http://dx.doi.org/10.1080/15216540500078962>.
 38. Weisel JW, Nagaswami C. Computer modeling of fibrin polymerization kinetics correlated with electron microscope and turbidity observations: clot structure and assembly are kinetically controlled. *Biophys J*. 1992; 63(1):111-28, [http://dx.doi.org/10.1016/S0006-3495\(92\)81594-1](http://dx.doi.org/10.1016/S0006-3495(92)81594-1).
 39. Ostman A, Thyberg J, Westermar KB, Heldin CH. PDGF-AA and PDGF-BB biosynthesis: proprotein processing in the Golgi complex and lysosomal degradation of PDGF-BB retained intracellularly. *J Cell Biol*. 1992; 118(3):509-19, <http://dx.doi.org/10.1083/jcb.118.3.509>.
 40. Herpin A, Lelong C, Favrel P. Transforming growth factor-beta-related proteins: an ancestral and widespread superfamily of cytokines in metazoans. *Dev Comp Immunol*. 2004;28(5):461-85, <http://dx.doi.org/10.1016/j.dci.2003.09.007>.
 41. Rinderknecht E, Humbel RE. The amino acid sequence of human insulin-like growth factor I and its structural homology with proinsulin. *J Biol Chem*. 1978;253(8):2769-76.
 42. He L, Lin Y, Hu X, Zhang Y, Wu H. A comparative study of platelet-rich fibrin (PRF) and platelet-rich plasma (PRP) on the effect of proliferation and differentiation of rat osteoblasts *in vitro*. *Oral Surg Oral Med Oral Pathol Oral Radiol Endod*. 2009;108(5):707-13, <http://dx.doi.org/10.1016/j.tripleo.2009.06.044>.